

ERIS: A Snapshot of the Guaranteed Time Programmes

Ric Davies¹
 Guido Agapito²
 Alex Agudo Berbel¹
 Andrea Baruffolo³
 Elena Bertola²
 Martin Black⁴
 Marco Bonaglia²
 Guillaume Bourdarot¹
 Runa Briguglio²
 Yixian Cao¹
 Luca Carbonaro²
 Giovanni Cresci²
 Yigit Dallilar⁵
 Quirino D'Amato²
 Matthias Deysenroth¹
 Ivan Di Antonio⁶
 Amico Di Cianno⁶
 Gianluca Di Rico⁶
 David Doelman⁷
 Mauro Dolci⁶
 Frank Eisenhauer^{1,10}
 Simone Esposito²
 Daniela Fantinel³
 Davide Fedele²
 Debora Ferruzzi²
 Helmut Feuchtgruber¹
 Natascha M. Förster Schreiber¹
 Reinhard Genzel¹
 Stefan Gillessen¹
 Adrian Glauser⁸
 Paulo Grani²
 Michael Hartl¹
 Jean Hayoz⁸
 David Henry⁴
 Heinz Huber¹

Christoph Keller⁷
 Matthew Kenworthy⁷
 Kateryna Kravchenko¹
 Harald Kuntschner⁹
 John Lightfoot⁴
 David Lunney⁴
 Dieter Lutz¹
 Michael Macintosh⁴
 Francesco Maio²
 Filippo Mannucci²
 Thomas Ott¹
 David Pearson⁴
 Alfio Puglisi²
 Sascha P. Quanz⁸
 Sebastian Rabien¹
 Christian Rau¹
 Armando Riccardi²
 Bernardo Salasnich³
 Hans-Martin Schmid⁸
 T. Taro Shimizu¹
 Frans Snik⁷
 Eckhard Sturm¹
 Linda Tacconi¹
 William Taylor⁶
 Hannah Übler¹
 Angelo Valentini⁶
 Christopher Waring⁴
 Marco Xompero²
 Maria V. Zanchettin²

¹ Max Planck Institute for extraterrestrial Physics, Garching, Germany

² INAF–Arcetri Astrophysical Observatory, Florence, Italy

³ INAF–Padua Astronomical Observatory, Italy

⁴ STFC UK ATC, Royal Observatory Edinburgh, UK

⁵ I. Physikalisches Institut, University of Cologne, Germany

⁶ INAF–Abruzzo Astronomical Observatory, Teramo, Italy

⁷ Leiden Observatory, Leiden University, The Netherlands

⁸ ETH Zurich, Institute for Particle and Astrophysics, Switzerland

⁹ ESO

¹⁰ Technical University of Munich, Germany

The Enhanced Resolution Imager and Spectrograph (ERIS) was conceived as a project to retain and enhance ESO's fundamental capabilities for diffraction-limited imaging and spectroscopy at ESO's Very Large Telescope. It significantly improves on the performance of two instruments that were being maintained beyond their operational lifetimes. The observational modes are integral field spectroscopy at 1–2.5 μm , imaging at 1–5 μm with several options for high-contrast imaging, and long-slit spectroscopy at 3–4 μm . ERIS has been in operation for the community since April 2023 and is very much in demand, regularly providing data quality that previously was only achieved in the best conditions. Here we highlight a snapshot of a few of the Guaranteed Time Observations projects, showing that the consortium is now engaged in an exciting science programme.

ERIS in a nutshell

The Enhanced Resolution Imager and Spectrograph (ERIS; Davies et al., 2023) is a Cassegrain instrument on Unit Telescope 4 of ESO's Very Large Telescope (VLT) that combines a new imaging camera (NIX), with a refurbishment and upgrade of the integral field spectrometer (SPIFFIER), and a new

Figure 1. The integration team after successfully mounting ERIS to the Cassegrain focus of Unit Telescope 4 at the VLT. Adhering to the restrictions associated with the pandemic, both for travel and while at the observatory, made the whole process of integration and testing much more arduous than in normal times.



adaptive optics module that makes use of the Adaptive Optics Facility (AOF). Phase B of the project began at the end of 2014 with a mandate from the ESO Scientific Technical Committee that the project should be aiming for first light not later than 2020. This goal was, however, largely stymied by the pandemic, which led to a severe restriction of lab access, hampered participation at acceptance tests and curtailed travel. Despite these challenges, the instrument was shipped in 2021 and integration at the observatory began immediately after international travel restrictions were lifted. Commissioning was carried out during 2022 (Figure 1), with a first light announcement¹ and then science verification at the end of that year (Concas et al., 2023). ERIS was included in the Call for Proposals for Period 111, with guest observations beginning in April 2023.

Figure 2. The Galactic Centre in *K*-band continuum (top left) and 2.17- μ m Br γ line emission (top right). The orbits of the three gas clumps are shown in the bottom panel, where they have been fitted simultaneously.

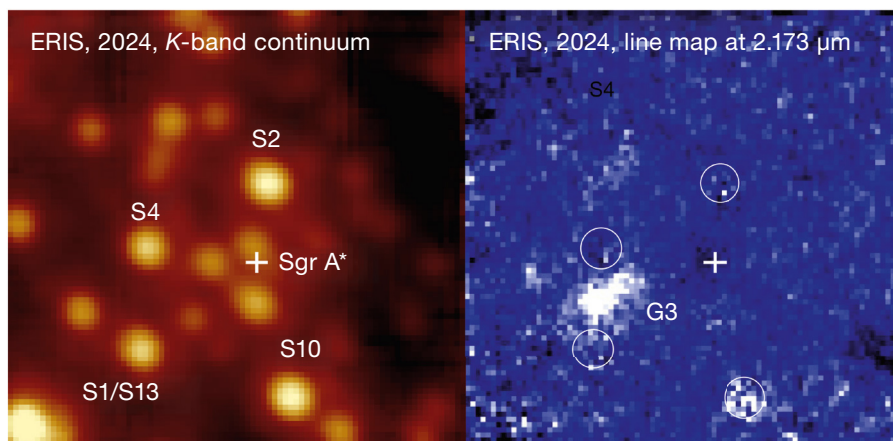
ERIS comprises several major sub-systems which are integrated in and around a central structure that attaches to the telescope adaptor-rotator:

- The Adaptive Optics module provides wavefront sensing and works with the AOF to correct atmospheric turbulence using the telescope’s deformable secondary mirror. With a natural guide star it can provide Strehl ratios up to about 80% in the *K* band in median conditions; and with a single laser guide star (from any of the four AOF lasers) it can reach 60% in the *K* band in median seeing, and has been tested with tip-tilt stars as faint as 19 mag in the *R* band.
- The Calibration Unit allows internal calibration and registration of the wavefront sensors at optical wavelengths, and the two science instruments at 1–2.5 μ m. Longer wavelength calibrations for NIX are performed on-sky.
- The integral field spectrometer SPIFFIER operates at 1–2.5 μ m and provides 64 \times 32 spatial pixels at 12.5 \times 25 milliarcseconds over a 0.8-arcsecond field,

50 \times 100 milliarcseconds over a 3.2-arcsecond field, or 125 \times 250 milliarcseconds over a 8.0-arcsecond field. It offers two spectral resolutions, $R \sim 5000$ over full bands, or $R \sim 10\,000$ over half bands.

- The imager NIX operates at 1–5 μ m and provides two pixel scales, 13 milliarcseconds over a 26.4-arcsecond field, or 27 milliarcseconds over a 55.4-arcsecond field. Imaging is offered with broad- and narrow-band filters, and with slow and fast speeds for reading the detectors. The observing modes include high-contrast imaging with a focal plane mask (annular groove, or vortex, mask) or pupil-plane masks (a grating vector apodised phase plate, or sparse-aperture masks), as well as long-slit for *L*-band spectroscopy at $R \sim 450$.

The consortium that designed and built ERIS together with ESO was led by the Max Planck Institute for extraterrestrial Physics, with the Italian National Institute for Astrophysics (INAF, at Arcetri, Teramo [now Abruzzo] and Padua), the UK Science and Technology Facilities Council (UK Astronomy Technology Centre, Edinburgh), the Swiss Federal Institute of Technology (ETH Zurich), and the Netherlands Research School for Astronomy (at Leiden). They provided the staff effort and contributed to the hardware costs, in return for which they were granted Guaranteed Time Observations (GTO). For these institutes the main science drivers were the Galactic centre, the evolution of galaxies, and exoplanets and their formation. The remainder of this article describes some of the initial results from the GTO programmes which are based on these themes.



Gas clouds in the Galactic centre

An unexpected and exciting discovery that for the first time provides a unified origin for all the reported detections of gas clouds in the Galactic centre (GC) was presented by Gillessen et al. (2026). The first detection of a gas cloud falling towards the GC just over a decade ago (Gillessen et al., 2012) led to a frenzy of activity to try and understand what it is and where it came from, and whether it would be dramatically disrupted as it passed close to SgrA*. In the end, there

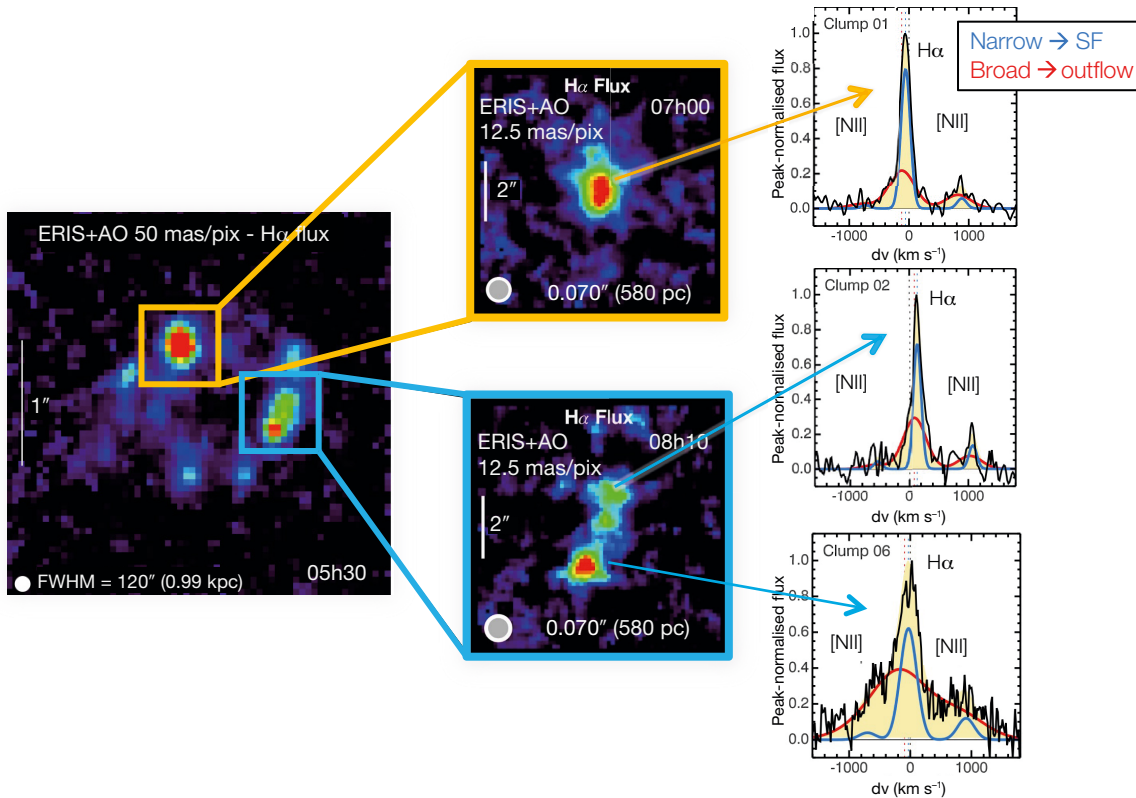


Figure 3. Eris/IFS+AO H α emission-line map of a clumpy galaxy at $z \sim 2.2$. The intermediate-resolution map obtained with the 50-milliarcseconds pixel $^{-1}$ scale (left) reveals a large number of faint clumps that match up well with JWST continuum imaging, as well as two brighter conglomerates. High-resolution mapping using the 12.5-milliarcseconds-pixel $^{-1}$ scale of these reveals their internal structures, and their spectral line profiles indicate both star formation and outflow.

was no firm consensus as to whether it was a pure gas cloud or had a stellar object at its centre, and it remained coherent even after pericentre which allowed the drag force of the interstellar medium to be measured. But it did lead to a retrospective realisation that a source emitting in the L band that had been noted a decade earlier was, after finding it in earlier Spectrograph for INtegral Field Observations in the Near-Infrared (SINFONI) datacubes, also a gas cloud with a similar orbit (Pfuhl et al., 2015). Now, within months of Eris being pointed towards the GC, a third gas cloud on a similar orbit has been discovered via its Br γ emission, creating a series G1-2-3 (Figure 2).

Because the likelihood of finding three clouds on similar orbits is low, Gillissen et al. (2026) modelled them with the same orbit, only allowing the time and longitude of pericentre to vary between them. The remarkable success of this endeavour strongly points to a common origin for all three clouds. And, indeed, the location and time of apocentre, and its implied rotation rate, are a close match to the orbit of IRS 16SW. This source is a Wolf-

Rayet eclipsing binary system that is known to have a stellar wind. Using smoothed-particle hydrodynamic simulations, the authors showed that in principle such a wind with a terminal velocity of 300–400 km s $^{-1}$ could interact with the ambient interstellar medium and form a dense bow shock. This then fragments into clumps, a few of which can end up on orbits towards Sgr A*. Further confirmation of this hypothesis is needed to understand the entire process better. And as monitoring of the GC continues, the picture will become clearer, perhaps leading to discovery of a fourth gas cloud in the coming decade.

Eris has also proven to excel when it comes to monitoring stellar orbits. The higher Strehl ratio compared to SINFONI has made it possible to classify a few faint stars in the direct vicinity of Sgr A*, which previously have not been accessible. The resulting radial velocities are very valuable: for stars with an astrometric acceleration, a single-epoch detection of the radial velocity uniquely determines the orbit. The high-resolution mode has also already yielded new insights: radial velocities of cooler stars with CO band-

heads in the K band can be determined with accuracies of around 1 km s $^{-1}$. This also translates directly into being able to determine orbits, because a change in radial velocity — a radial acceleration — is as valuable as an astrometric one.

Zooming in on the clumps of cosmic noon galaxies

It is nearly two decades since near-infrared integral field spectroscopy showed the first evidence, by tracing spatially resolved line emission and kinematics, that a majority of star-forming galaxies at $z \sim 2$ were rotating discs, despite prominently clumpy morphologies especially towards rest-frame ultraviolet wavelengths. Subsequent deep adaptive optics observations of increasing numbers of star-forming galaxies at cosmic noon resolved the ionised gas, via the H α and [NII] lines, on similar scales, revealing their detailed morphology and kinematics (Förster Schreiber et al., 2018 and references therein). However, probing the internal structure of the clumps themselves had to wait for the higher throughput and better adaptive optics performance of Eris.

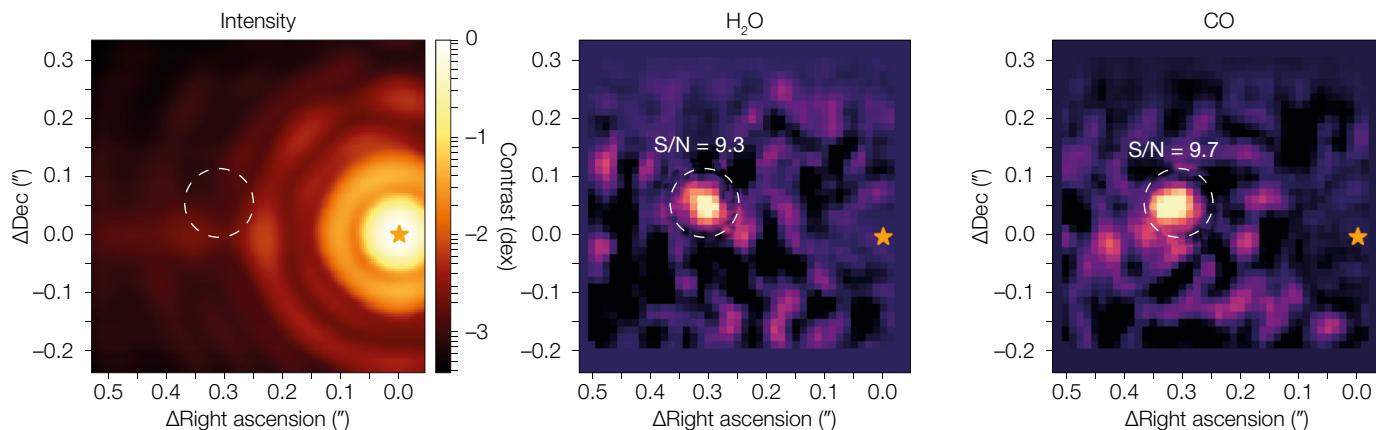


Figure 4. Molecular mapping of AF Lep b with integral field spectroscopy. Left: continuum image of the star, with the location of the planet marked. Centre & right: cross-correlation maps of the H₂O and CO respectively, showing a clear detection of the planet.

Very deep integrations, of 10–20 hours, together with careful compensation of the residual flexure and special techniques for reducing the impact of the OH night sky lines, have yielded data with spatial resolution close to 500 pc. They show that rather than all having condensed out of the global kinematics, the clumps exhibit a variety of structures with at most modest internal kinematic signatures and a wide range of masses, star formation rates and outflow rates (for example, Förster Schreiber et al., 2026). Data for one clumpy galaxy at $z = 2.19$ are featured in Figure 3. In this case the brightest clump has a compact core but also a rather smooth envelope extending out to a kiloparsec, and another clump appears to have two compact cores close to each other without a broader halo. In a third case, the ionised gas complex is resolved in a string of compact clumps that contrasts surprisingly with the shorter wavelength continuum images from JWST at comparable resolution, suggestive of a range of evolutionary ages. The spectral profile of the line emission reveals outflows that in one case dominate the line profile and can be traced to velocities exceeding 1000 km s^{-1} . The mass, star formation rate and outflow rate of this particular clump show that this extreme and off-centre star cluster may host an accreting black hole.

Molecular mapping of exoplanets

A very different application of integral field spectroscopy, that has been around for about a decade, is to directly test for the presence of molecules in the atmospheres of exoplanets, which simultaneously provides a measure of the radial velocity and hence helps pin down the orbital parameters. The first demonstration of how successful this technique can be with ERIS was made by Hayoz et al. (2025) for the young super-Jovian planet AF Lep b. This planet, which is at a distance of 27 pc and orbits an F8V star, has a mass of only $3.7 \pm 0.5 M_{\text{Jup}}$ putting it among the lowest-mass exoplanets that have been directly imaged.

Achieving the result required developing techniques suited to this type of data to improve on the wavelength calibration provided by the pipeline. Using the $R \sim 11\,000$ resolution to exploit differences in spectral features between the star and its companion, the stellar spectrum was then removed from the data cube. The residuals contain key information about the planet’s atmosphere, which can be extracted by cross-correlation with molecular spectral templates, making use of all the spectral channels simultaneously. Doing this for H₂O and CO yielded very significant detections in the same location (Figure 4), while CH₄ and CO₂ were not detected. Since the planet’s temperature of 800 K would tend to favour CH₄ over CO, this result supports the hypothesis of chemical disequilibrium in which there is an upward stream from hotter deeper layers bringing molecules such as CO to the surface.

The cross-correlation technique simultaneously provides a measure of the radial velocity of the planet with respect to the star via the spectral location of its peak. The relative velocities associated with the two detected molecules are $8.9 \pm 2.5 \text{ km s}^{-1}$ and $6.1 \pm 2.8 \text{ km s}^{-1}$. These values are consistent with an independent measurement from the High-Resolution Imaging and Spectroscopy of Exoplanets (HiRISE; Denis et al., 2025) instrument at the Very Large Telescope and unambiguously favour an orbital solution in which the planet was close to its maximum line-of-sight velocity, recently crossing the plane of the sky so that it is currently located behind the star. This means it is now possible to compute a phase curve for AF Lep b, which is important for planning future visible observations that probe the reflected light. A follow-up work (Hayoz et al., 2026) applying the same technique to 12 planetary-mass companions has ubiquitously detected H₂O and CO in their atmospheres, and enabled the detection of the ¹³CO isotopologue in one of them. Combined with archival data, the new ERIS spectra were able to systematically constrain the atmospheric C/O ratio and metallicities of these companions, yielding insights into planet formation scenarios. And in addition the radial velocities and relative astrometry have improved the constraints on their orbital parameters.

A mid-infrared view of protoplanetary discs

Detecting embedded protoplanets remains extremely challenging because

these young objects are deeply buried within their natal discs, where strong dust extinction and bright stellar residuals hinder direct detection. High-contrast imaging in the L' band offers a powerful way to overcome these limitations by reducing the impact of local extinction and enhancing the planet-to-star flux contrast, making it one of the most promising techniques to reveal forming planets. To enable this, ERIS has a grating vector Apodizing Phase Plate (gvAPP) mounted in the pupil plane, the laboratory and on-sky performance of which are thoroughly analysed by Kenworthy et al. (2026), and also an annular-groove phase mask (vortex coronagraph) mounted in the focal plane.

Using the gvAPP, Maio et al. (2025a) detected seven protoplanetary discs, including two without previous $4\text{-}\mu\text{m}$ detections. In a companion paper using the vortex mask, Maio et al. (2025b) focused on the HD 135344B system, a well-studied transitional disc located at 136 pc and characterised by a wide (~ 40 au) cavity, multiple optical/near-infrared spiral arms, and a striking azimuthal asymmetry at millimetre wavelengths. As shown in their press release², the ERIS data recover the known S1, S2, and S2a spirals, confirming the rich substructure of the disc. Beyond these previously identified components, the data reveal a new point source embedded in the inner disc at the base of the S2 spiral, located about 28 au from the star. The source displays an L' -band contrast of around 3×10^{-3} , and the multi-wavelength analysis suggests a mass $\geq 2 M_{\text{Jup}}$ together with significant dust extinction ($A_V \geq 10$ mag). Its strong L' emission combined with non-detections at shorter wavelengths is consistent with an actively accreting proto-planet sur-

rounded by a circumplanetary disc. Additionally, a previously unrecognised spiral arm was identified to the northwest, further enriching the morphological complexity of the system. Taken together, these results point toward a physical connection between the detected proto-planet candidate and the surrounding disc substructures, and they provide compelling support for a planet-driven origin of the cavity and spirals in HD 135344B.

Active galactic nuclei: outflows, black hole binaries, and lenses

Active galactic nuclei (AGN) play a crucial role in shaping the evolution of galaxies at all cosmic times through various feedback mechanisms, with impacts on our understanding of galaxy evolution models, particularly at the low- and high-mass ends, and whether galaxies and their supermassive black holes (SMBHs) co-evolve. The extended sky coverage reached by ERIS allows larger populations to be observed at the diffraction limit, enabling a variety of opportunities, including spatially resolving ionised outflows at redshift $z = 2\text{--}11$ in galaxies where the molecular gas content is known, in order to assess whether the outflow properties correlate with the available gas reservoirs (Bertola et al., 2026). A second project aims to build a bridge between cosmological simulations of galaxy evolution and the predictions for gravitational wave events from SMBH mergers, by quantifying the incidence of the dual-AGN phase of galaxy evolution, when two or more SMBHs co-exist in a single post-merger galaxy. The merging timescales of these SMBHs can be up to several Gyr and during this phase the

objects are revealed as pairs of AGN at close separations (1–6 kpc) inside a common host galaxy. The high angular resolution afforded by ERIS is used to classify the systems as dual or lensed AGN (Mannucci et al., 2023). Figure 5 shows an example of dual AGN separated by 2.2 kpc, with distinct spectra for the two QSOs (Zanchettin et al., 2026). Cases where the systems are identified as lensed QSOs also yield key results, as in the beautiful case of the most compact quadruply lensed QSO known, with an Einstein radius of only 0.2 arcseconds (D’Amato et al., 2026). The background QSO at $z = 2.79$ is lensed by a foreground galaxy at $z = 1.05$, the mass of which can be ascertained rather precisely as $2.3 \times 10^{10} M_{\odot}$. The high fidelity of the image allows the galaxy profile and luminosity to be measured, showing that it is an early-type galaxy. The mass-to-light ratio strongly favours a Chabrier IMF, providing one of the best IMF constraints to date on a low-mass galaxy at this redshift.

Final Note

The highlights above represent a current snapshot of some of the GTO projects that the ERIS consortium is pursuing. Contributing to the design, construction, and commissioning of an instrument requires a significant investment of effort over many years. The increasing number of partners in such projects means that an ever larger part of the community can benefit from the GTO which compensates that investment during the first few years of operation, sometimes through programmes that wouldn’t necessarily be possible through the open time proposal channel. Similarly, the high demand for

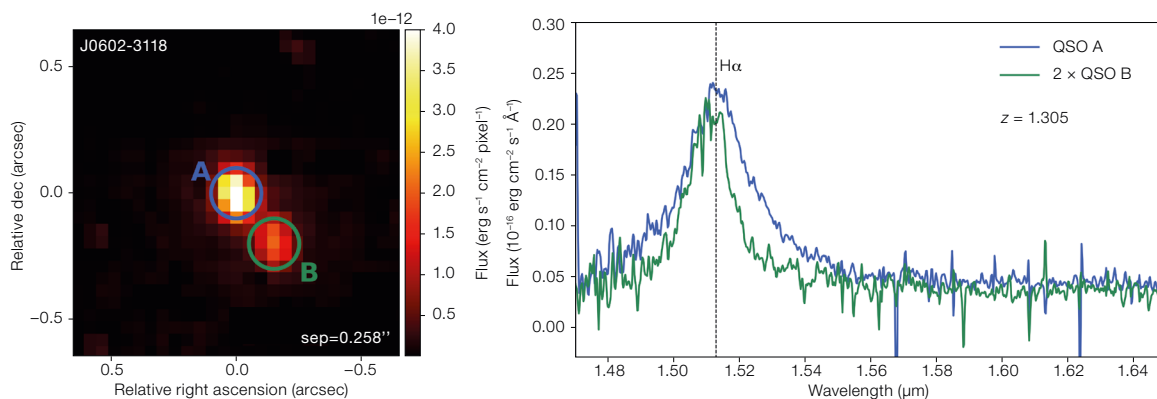


Figure 5. ERIS integral field spectroscopy provides an image (left) and spectra (right) of the two components of the dual AGN J0602-3118 at $z = 1.305$. Even for a projected separation between the two AGN of only 0.258 arcseconds, ERIS can obtain well-resolved spectra, allowing for a clear classification of the system.

ERIS shows that community is also benefiting from the novel capabilities of this new instrument.

Acknowledgements

The consortium would like to thank the many people who have contributed to the project in numerous different ways, in some cases ‘behind the scenes’, both within the partner institutes and at ESO in Garching and at Paranal.

References

- Bertola, E. et al. 2026, in preparation
 Concas, A. et al. 2023, *The Messenger*, 191, 25
 D’Amato, Q. et al. 2026, *Nat. Astron.*,
<https://doi.org/10.1038/s41550-026-02819-4>
 Davies, R. et al. 2023, *A&A*, 674, A207
 Denis, A. et al. 2025, *A&A*, 696, A6
 Förster Schreiber, N. M. et al. 2018, *ApJS*, 238, 21
 Förster Schreiber, N. M. et al. 2026, in preparation
 Gillessen, S. et al. 2025, *A&A*, 707, A79
 Gillessen, S. et al. 2012, *Nature*, 481, 51
 Hayoz, J. et al. 2025, *A&A*, 698, A87
 Hayoz, J. et al. 2026, *A&A*, 708, A312
 Kenworthy, M. et al. 2026, *A&A*, 708, A239

- Maio, F. et al. 2025a, *A&A*, 698, A52
 Maio, F. et al. 2025b, *A&A*, 699, L10
 Mannucci, F. et al. 2023, *A&A*, 680, A53
 Pfuhl, O. et al. 2015, *ApJ*, 798, 111
 Zanchettin, M.V. et al. 2026, in preparation

Links

- ¹ Sharper infrared eyes for the VLT: ERIS sees first light <https://www.eso.org/public/announcements/ann22015>
² A disc and a planet candidate around the star HD 135344B <https://www.eso.org/public/images/comparisons/eso2513a>



This image shows the full scope of Paranal's beauty. Cerro Paranal in Chile's Atacama Desert, the mountain peak home to ESO's Very Large Telescope (VLT), is a site of many marvels. And this panoramic image taken by Chilean astrophotographer Alexis Trigo certainly captures them all.

Right in front, one of the movable Auxiliary Telescopes (ATs) stands tall. While this “relatively” small 1.8-m telescope has its eyes shut, its bigger siblings, the Unit Telescopes (UTs), each with an 8.2-m mirror, are scanning the sky. The lasers emerging from the UTs each create a bright artificial star on the sky, so the shifts and swirls of the atmosphere can be measured and corrected to deliver sharp data.